

## ASSESSMENT OF THE Fe–Sn–Zn PHASE DIAGRAM AT 450°C Application to the batch galvanizing

Marie-Noelle Avettand-Fènoël<sup>1\*</sup>, N. David<sup>2</sup>, G. Reumont<sup>1</sup>, J.-M. Fiorani<sup>2</sup>, M. Vilasi<sup>2</sup>  
and P. Perrot<sup>1</sup>

<sup>1</sup>Laboratoire de Métallurgie Physique et Génie des Matériaux, U.M.R. C.N.R.S. 8517, Université de Lille 1  
59650 Villeneuve D'Ascq, France

<sup>2</sup>Laboratoire de Chimie du Solide Minéral, U.M.R. C.N.R.S. 7555, Université Henri Poincaré, Nancy I  
54506 Vandoeuvre Les Nancy, France

The Fe–Sn–Zn system is of interest because Sn is one element added to the Zn galvanizing bath to overcome the drawbacks due to the presence of Si in semi-killed steels. This work has been undertaken with the aim to understand the tin effect on the microstructure and the layers growth in batch galvanized coatings on low alloyed steels.

Various experimental techniques such as metallography, scanning electron microscopy (SEM) coupled with X-ray energy dispersive spectroscopy (EDX) are used in order to characterize the microstructure and the properties of such coatings elaborated in a zinc bath enriched with tin.

Solidification phenomena and layers growth mechanisms during galvanization are explained by means of the ternary phase diagram Fe–Sn–Zn at 450°C. The Calphad method allows to obtain this phase diagram from the three optimized binary phase diagrams Fe–Sn, Fe–Zn and Sn–Zn and some experimental data inside the ternary Fe–Sn–Zn system.

**Keywords:** batch galvanizing, Calphad method, Fe–Sn–Zn diagram

### Introduction

During galvanizing, silicon present in steels forms reactive coatings leading to overthickness, poor surface appearance and delamination. This phenomenon is known as Sandelin effect [1]. Various means such as an addition of nickel, manganese, aluminium or tin [2–5] are developed in order to reduce the reactivity of such steels. For this reason, the Fe–Sn–Zn system, unknown till now, has raised our interest with the aim to modelize the interaction of Si semi-killed steels with zinc bath enriched with tin [6].

In present work, we investigate the role of tin during batch galvanizing on the coatings microstructure and the formation of galvanized layers at 450°C, classical temperature of galvanizing.

### Experimental

One silicon free steel substrate has been utilized. Its chemical composition, determined by means of a glow discharge spectroscopy device (LECO-GDS 850A) is

shown in Table 1. Steel samples were pickled in an acid solution (50% hydrochlorhydric acid with 3% of hexamethylenetetramine acting as a corrosion inhibitor), cleaned in water, then fluxed in a solution constituted of 100 g L<sup>-1</sup> of ammonium chloride and of 100 g L<sup>-1</sup> of zinc chloride in water and finally dried.

Samples were batch galvanized, as prepared. They were dipped at 450°C for 9 min in a zinc bath with tin additions (<5 mass%) and saturated with iron. Then they were cooled under air.

Cross sections of batch galvanized samples were hot embedded in an enriched carbon resin and polished to 1 μm.

Etching in a nital 4% solution for 5 s allowed to reveal the various layers of galvanized coatings. Their morphology and chemical nature were characterized by optical microscopy, and with a scanning electron microscope (SEM) F.E.I. Quanta 400 equipped with an energy dispersive spectroscopy (EDX) device and operating under 20 kV.

The phase diagrams assessment by the Calphad method allows a useful discussion of metallurgical phenomena [7].

**Table 1** Mass composition of low alloyed steel substrate determined by luminescent discharge spectroscopy

Fe/%	C/%	Mn/%	P/%	S/%	Cu/%	Ni/%	Cr/%	Al/%	Zr/%
99.600	0.034	0.228	0.012	0.005	0.012	0.024	0.027	0.052	0.001

\* Author for correspondence: Marie-Noelle.Avettand-Fenoel@univ-lille1.fr

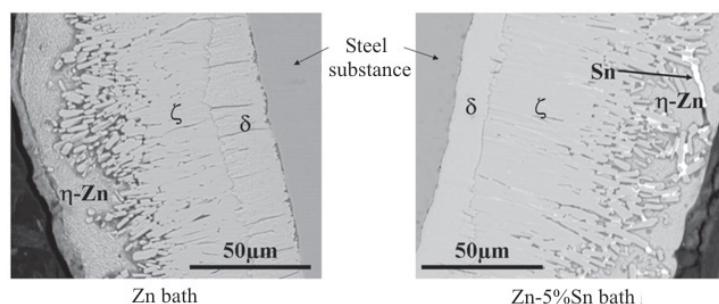


**Fig. 1** Effect of tin added to the galvanizing bath on the morphology of coatings obtained on low alloyed steel substrates (BSE/SEM micrographs). Tin is the white phase

## Results and discussion

Some back scattered electrons (BSE)/SEM micrographs of the coatings for various tin contents introduced in the bath are shown in Fig. 1. EDX analyses indicate that the coating is composed of two intermetallic compounds  $\delta$  and  $\zeta$  and of the  $\eta$ -Zn phase. Tin (in white on BSE/SEM micrograph) is rejected by Zn and trapped at the interface between  $\delta$  and  $\zeta$ , between the columnar grains of  $\zeta$  compound and in the  $\eta$ -Zn phase (Figs 1 and 2). No solubility of tin in  $\delta$ ,  $\zeta$  and  $\eta$ -Zn phases was detected by EDX analyses.

Calphad method allowed to assess the binary phase diagrams Fe–Sn, Fe–Zn (Zn-rich part) and Sn–Zn (Figs 3a–c) by means of different data bases [8–12]. The phase diagram Sn–Zn presented in Fig. 3c shows that tin has no solubility in zinc. Iron forms with tin and zinc many intermetallic compounds (Figs 3a and b).

The assessment of the Fe–Sn–Zn ternary phase diagram at 450°C (Fig. 3d) has been achieved by using 1) stoichiometric binary description of intermetallic compounds where a ternary solubility has been considered in relation with the atomic substitution and 2) a part of the experimental results of Tang *et al.* [13]. Moreover, it has just been considered the boundaries Fe–Sn, Fe–Zn and Sn–Zn in agreement with the binary phase diagrams at 450°C. The assessed parameters are summarized in Table 2.

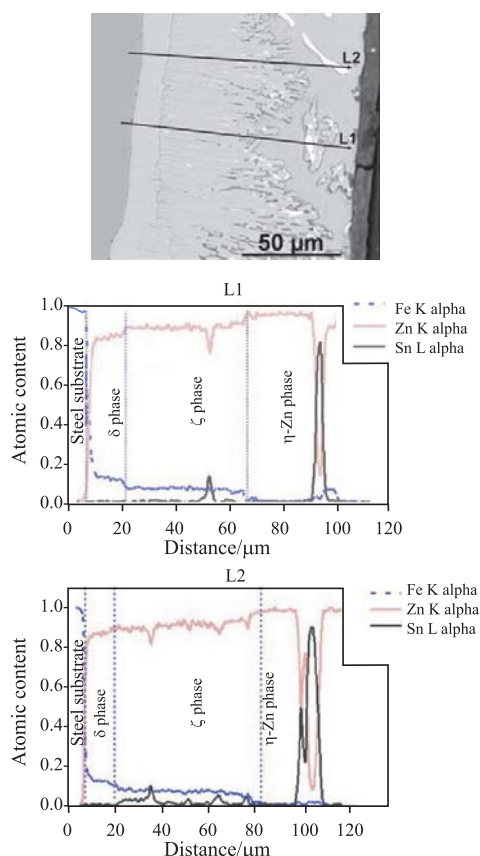


**Fig. 2** BSE/SEM micrograph of a coating elaborated in a bath of Zn–5 mass% Sn and profiles of concentration corresponding to the analyses lines L1 and L2 (EDX)

**Table 2** Calphad assessment of the 450°C isothermal section Fe–Sn–Zn phase diagram ( $T$  in K)

Phase	Assessed parameters	Value/ $\text{J mol}^{-1}$
Liquid	L0 (liquid, Fe, Sn, Zn)	20004
FeSn	G (FeSn, Fe:Sn)	$-48072+34.914T$
(Fe,Zn)(Sn)	G (FeSn, Zn:Sn)	1200
FeSn <sub>2</sub>	G (FeSn <sub>2</sub> , Fe:Sn)	$-77818+67.826T$
(Fe,Zn)(Sn) <sub>2</sub>	G (FeSn <sub>2</sub> , Zn:Sn)	0
$\delta$	G ( $\delta$ , Fe:Zn)	$-5418.06133+1.57837323T$
(Fe,Sn) <sub>0.125</sub> (Zn) <sub>0.875</sub>	G ( $\delta$ , Sn:Zn)	-750
$\Gamma_2$	G ( $\Gamma_2$ , Fe:Zn)	$-7324.97391+3.02901415T$
(Fe,Sn) <sub>0.2</sub> (Zn) <sub>0.8</sub>	G ( $\Gamma_2$ , Sn:Zn)	-1600
$\zeta$	G ( $\zeta$ , Fe:Zn)	$-4507.81256+2.02071265T$
(Fe,Sn) <sub>0.072</sub> (Zn) <sub>0.928</sub>	G ( $\zeta$ , Sn:Zn)	19462

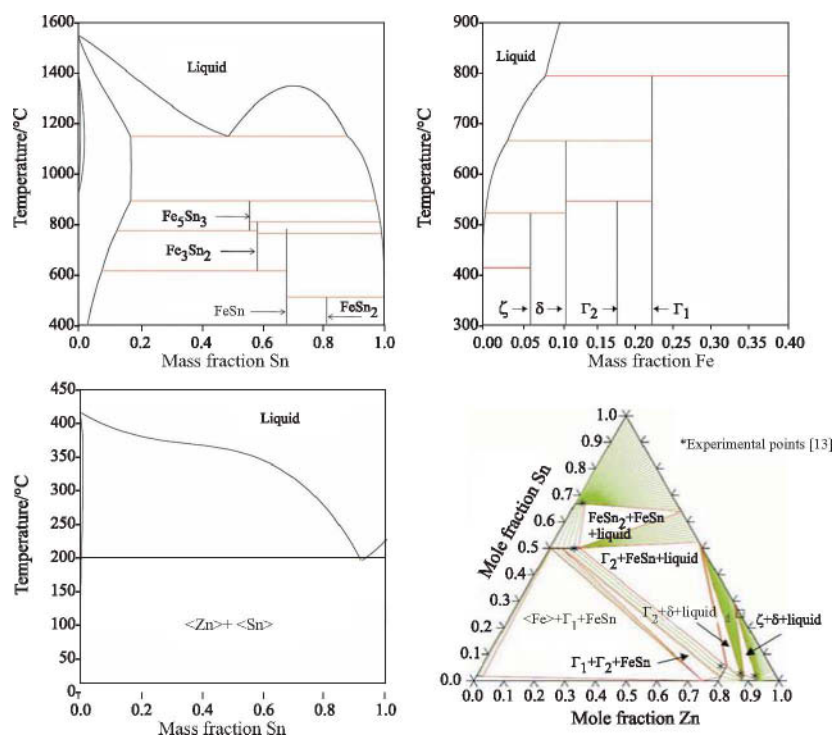


Fig. 3 Assessment of a – Fe–Sn, b – Fe–Zn, c – Sn–Zn and d – Fe–Sn–Zn phase diagram at 450°C

The main points of the experimental results can be summarized as follows:

- The ratio between zinc and tin contents in the bath can explain the formation of  $\delta$  and  $\zeta$  phases.
- Tin solubility in pure solid zinc and in Fe–Zn intermetallic compounds is hardly detectable, that means less than 0.5 at. %.
- Although Zn–Sn systems gives an eutectic ([14] and Fig. 2c), cooling of coatings developed in baths enriched with Sn leads to pure Sn inclusions without appearance of a solid eutectic in the galvanizing coating. The presence of pure tin in galvanized coating could be explained by an undercooling of tin below the eutectic temperature. Tin remains the last phase that solidifies in the coating, which agrees with its rounded morphology.
- Literature data mention differential scanning calorimetry (DSC) experiments carried out on coatings (on Sandelin steel substrates) elaborated in a Zn bath with 1 mass% Sn [14]. A small shift of  $\eta$ -Zn phase temperature has been observed: it suggests a dissolution of other elements such as Fe (because galvanizing bath is saturated with Fe) and/or Sn in Zn or/and a small variation of the crystal structure of  $\eta$ -Zn phase [14]. Nevertheless Fe solubility in  $\eta$ -Zn phase at 450°C remains very low (about 0.035 at. %), which could not totally explain the temperature shift. A low solubility of Sn in  $\eta$ -Zn phase could then originate the  $\eta$ -Zn

phase temperature shift on DSC scans. Literature data [14] and our experimental results show that Sn solubility in  $\eta$ -Zn is low. Nevertheless the EDX analyses alone do not lead to the conclusion of an absence of solubility.

- When tin content in liquid phase increases, the following equilibria are successively obtained: liquid- $\zeta$ , liquid- $\delta$  and liquid-FeSn. In comparison with another work [13, 15], the assessed equilibrium between  $\delta$  and FeSn prohibits an equilibrium between  $\Gamma$  ( $\Gamma_1$  or  $\Gamma_2$ ) and liquid.
- The previously proposed solidification mechanism of galvanized coating [3] is experimentally confirmed by the presence of tin which plays a role of marker.

## Conclusions

Our optimization of the Fe–Sn–Zn system gives an insight on the phase equilibria at 450°C which justifies microstructural observations. When dipping steel in Zn–Sn liquid bath, the Fe–Zn intermetallic compounds, mainly  $\zeta$  and  $\delta$ , are formed. Subsequently, liquid Zn near the galvanizing layer is more enriched with Sn because  $\zeta$  and  $\delta$  are in equilibrium with Zn-5 mol% Sn liquid. Further cooling leads to the precipitation of quite pure tin in the coating.

**References**

- 1 R. Sandelin, *Wire and Wire Products*, 16 (1941) 28.
- 2 J. Foct, G. Reumont and P. Perrot, *The Minerals, Metals and Materials Society*, A. R. Marder, Ed., 1993, p. 1.
- 3 J. Foct, P. Perrot and G. Reumont, *Scripta Met. Mater.*, 28 (1993) 1195.
- 4 W. Katzung, Intergalva '97, 18<sup>th</sup> Intern. Galvanizing Conf., Birmingham 1997, 8p.
- 5 M. Gilles and R. Sokolowski, Intergalva '97, 18<sup>th</sup> Intern. Galvanizing Conf., Birmingham 1997, 8p.
- 6 M.-N. Avettand-Fènoël, G. Reumont P. Perrot, Intergalva, Naples 2006, 9p.
- 7 B. Sundman, B. Jansson and J. O. Andersson, *Calphad*, 9 (1985) 153.
- 8 N. David, Thesis, Université Poincaré: Nancy I, 22 juin 2001.
- 9 X. Su, N.-Y. Tang and J.-M. Toguri, *J. Alloys Compd.*, 325 (2001) 129.
- 10 V. Raghavan, *J. Phase Equilib.*, 24 (2003) 544.
- 11 B.-P. Burton and P. Perrot, *Phase Diagrams of Binary Iron Alloys*, Ed. ASM, 1989, p. 459.
- 12 G. Reumont, M. Mathon, R. Fourmentin and P. Perrot, *Z. Metallkde*, 94 (2003) 411.
- 13 N.-Y. Tang, X. Su and X. Bin Yu, *J. Phase Equilib.*, 24 (2003) 528.
- 14 N. Pistofidis, G. Vourlia, E. Pavlidou, K. Chrissafis, G. Stergioudis, E. K. Polychroniadis and D. Tsipas, *J. Therm. Anal. Cal.*, 86 (2006) 417.
- 15 V. Raghavan, *J. Phase Equilib. Diffusion*, 28 (2007) 399.

---

DOI: 10.1007/s10973-007-8386-z